ABSTRACT

VENUGOPAL, ARVIND. Analysis and Design of Microstrip antenna for a Smart-antenna test-bed. (Under the direction of Professor Gianluca Lazzi.)

Small planar antennas are becoming increasingly popular in personal wireless communication systems since these antennas offer advantages such as small size, light weight, robust construction, ease of integration into mobile handsets, reasonable radiation efficiency and gain. A new small microstrip antenna operating at 880MHz is designed using the Finite difference time domain technique incorporating the perfectly matched-layer formulation. Shorting pins are used to achieve the reduction in size. The size of this patch antenna is approximately four times less than that of the regular half wavelength patch antenna. An antenna array made of the new patch antennas is used in a multiple antenna system to reliably separate different users on the same channel using linear beam steering techniques with the ultimate goal of increasing the channel capacity. Prototypes of the proposed dual shorted-pin-patch antenna are fabricated and measurements of their return loss compare well with the computational results.

Analysis and Design of Microstrip antenna for a Smart-antenna test-bed

by

Arvind Venugopal

A thesis submitted to the Graduate Faculty of
North Carolina State University
in partial fulfillment of the
requirements for the degree of
Master of Science

Department of Electrical and Computer Engineering

Raleigh, NC
July 30, 2001

Approved By:

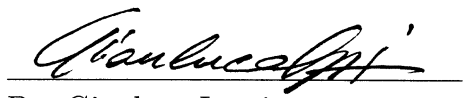

Dr. Gianluca Lazzi
Chair of Advisory Committee

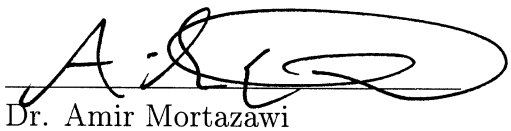

Dr. Amir Mortazawi

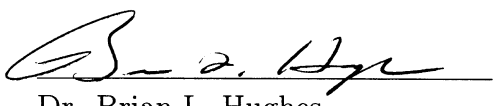

Dr. Brian L. Hughes

Biography

Arvind Venugopal was born in Kerala, India on Jan. 1st, 1977. He received the B.S. degree in Electrical Engineering from the University of Calicut, India. He came to North Carolina State University where he is currently working towards the Master of Science Degree in Electrical and Computer Engineering. His research interests includes Numerical techniques in Electromagnetics, RF circuits and Wireless Communications.

Acknowledgements

I would like to thank my committee chair, Dr.Gianluca Lazzi for his guidance and help in my research and also for the time and effort he invested on me, he has also been unfailing in helping me get the resources and information I needed to complete this research . I would also like to acknowledge and thank Dr. Amir Mortazawi and Dr. Brian L. Hughes for being on my thesis committee and offering their observations and suggestions. My acknowledgements also go to Dr. Christian Schlegel of University of Utah, Salt Lake City, for his valuable research suggestions.

I am also greatly indebted to Sean Christopher Ortiz, Mete Ozkar and Stephen Christopher Demarco for their support and help which enabled me to complete this project. They have been a constant source of knowledge for me.

Last but not least, I would like to thank my family and friends who have stood by me all this time.

Contents

List of Figures

Chapter 1

Introduction

The mobile wireless communications industry has grown by orders of magnitude, fueled by Digital and RF circuit fabrication improvements, VLSI technology, and antenna miniaturization technologies which make portable wireless equipment small, economical, and reliable. A successfully emerging trend in the wireless communications is the use of smart-antenna systems. A smart antenna system employs multi-element antenna arrays that can automatically adjust to a dynamic signal environment. Smart antenna systems also provides a substantial increase in the channel capacity of wireless systems. They offer the ability to improve signal reception and signal detection. The Radiation pattern for the antenna array can be formed in such a way that the main beam points to the desired signal and the nulls are directed towards the interferers. Furthermore, unlike the conventional communication systems, it is possible to increase throughput in a given spectrum by relying on the ability of the smart antenna to exploit the multi-path channel conditions to convey additional information. Until recently the cost and size of employing antenna array systems had inhibited their widespread use. However, with the development of economical methods which successfully limits the antenna-size, there is a surge of interest in developing and utilizing antenna array technologies. With the substantial benefits that the antenna array systems offer, it is inevitable that they will become an integral part of future wireless networks.

1.1 Multiple-antenna systems

The antenna-array systems can be categorized as follows:

Switched beam systems

These systems use an array of antennas that offer multiple fixed beams to the transmitter or the receiver, which then selects one beam which provides the maximum signal strength and reduces interference. The switched beam system selects one of several predetermined fixed-beam patterns with the greatest SNR for the user's channel. The system switches its beam in different directions throughout the space by changing the phase differences of the signals used to feed the antenna elements or received from them. When the mobile user enters a particular sector, the switched beam system selects that beam containing the strongest signal. Throughout the call, the system monitors signal strength and switches to other fixed beams as required. Hence switched beam antenna system can be considered as an array of multiple directional antennas with diversity combining as the process of selection of the best beam.

Adaptive antennas

This system has the ability to change antenna gain pattern dynamically to adjust to noise, interference and multi-paths and to adjust to mobile users. The adaptive array beamformer uses a weighted linear combination of the received signal vector components to form the output. This output detects the desired signal direction with maximum gain towards the direction of the desired signal i.e. the main lobe is directed towards the signal of interest. By adaptively changing the weights of the received signal's vector components, the beam can be steered towards a desired direction and at the same time place nulls or sidelobes in the direction of interference, thus simultaneously reducing co-channel interference . An adaptive antenna array directs its main lobe with enhanced gain in the direction of the user and forms side lobes and nulls which are the areas of medium and minimal gain respectively, in directions of the interference. Adaptive antenna systems control the lobes and the nulls with

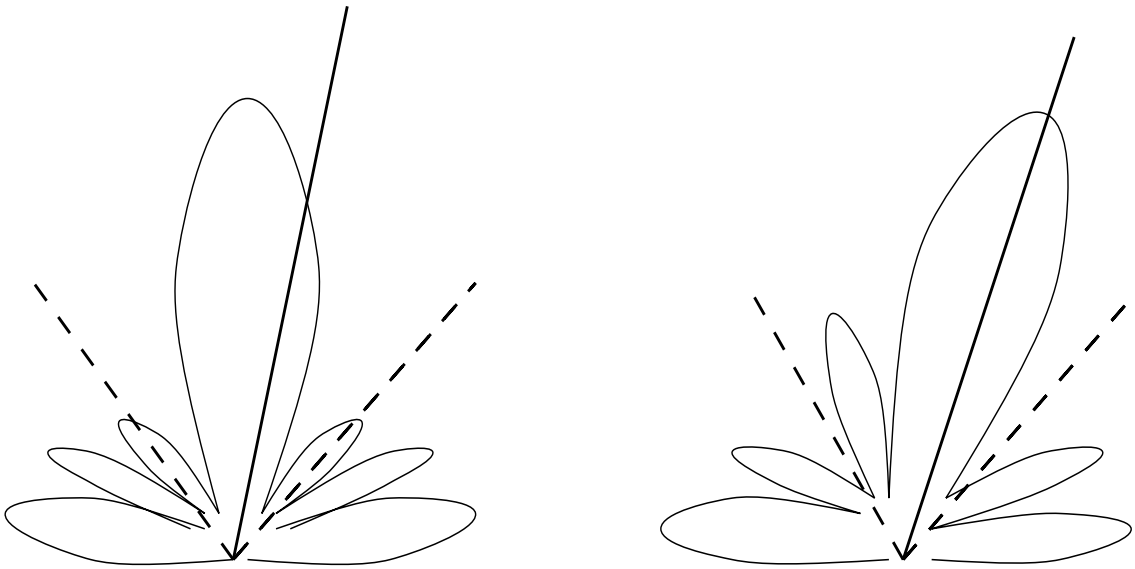

Figure 1.1: Switched and Adaptive Antenna Systems

varying degrees of accuracy and flexibility. Figure 1.1 illustrates the comparison of beampatterns for a switched beam system and a adaptive antenna system.

1.2 Space-Time diversity

A multiple antenna system can not only reliably separate different users on the same channel using beam steering techniques described above, it also increases the inherent capacity of link. This may mean, among other conditions, that the signals may have to be transmitted from different transmitter locations, or that multipath propagation is exploited as suggested by Bellcore's Blast project [1]. In wireless systems, radio waves do not propagate simply from transmit antenna to receive antenna, but bounce and scatter wildly off objects in the environment. This scattering is known as multipath, as it results in multiple copies or images of the transmitted signal arriving at the receiver via different scattered paths. In conventional wireless systems, multipath represents an impairment to accurate transmission, because the images arrive at the receiver at slightly different times and can thus interfere destructively, canceling

each other out. For this reason, multipath is traditionally viewed as a serious impairment. Using the BLAST approach however, it is possible to exploit multipath, that is, to use the scattering characteristics of the propagation environment to enhance, rather than degrade, transmission accuracy by treating the multiplicity of scattering paths as separate parallel subchannels. Since the early work by Shannon, it is well understood that channel capacity, the maximum reliable data rate that can be supported by a given channel, is an unmovable barrier. Increasing data rates beyond these limits is only possible by increasing the capacity of the transmission channel itself. One such method is the use of multiple transmit and receive antennas, generating parallel channels. Such multiple antenna systems can theoretically increase capacity by up to a factor equaling the minimum of the numbers of transmit and receive antennas used [2,3]. The channel model assumes t transmit and r receive antennas. Each antenna transmits n symbols from a complex symbol alphabet each with power ρ/t per signaling interval. These transmit symbols are modulated by a suitable pulse waveform and up-converted to the desired transmission band, in our case 800-900MHz, and transmitted over the t transmit antennas. At the receiver the signals from each receive antenna are down-converted to baseband, sampled, and fed into a field-programmable gate array (FPGA), which decodes the sampled signals using discrete signal processing algorithms. This basic system is illustrated in Figure 1.2.

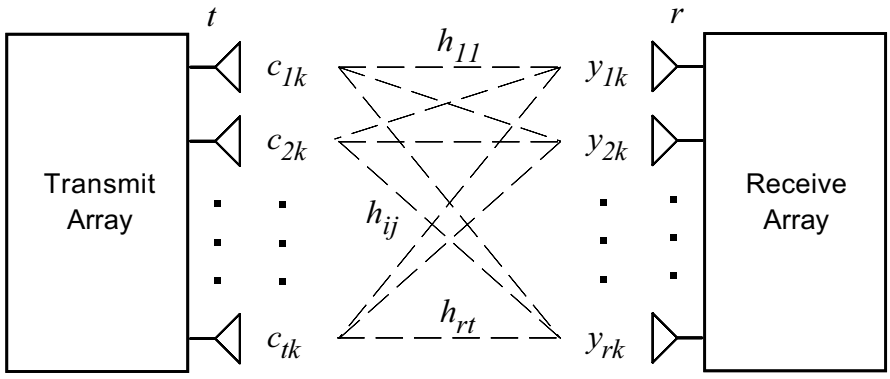

Figure 1.2: MIMO Channel model

The received sampled signal y_{jn} for the j^{th} receive antenna at time n is then given by

$$y_{jn} = \sum_{i=1}^{T} h_{ij} c_{in} \sqrt{\rho} + \eta_{jn}, \tag{1.1}$$

where η_{jn} is a sample of circularly symmetrical Gaussian noise with variance N_0, and h_{ij} is the complex *path strength* from transmit antenna i to receive antenna j. It contains all linear effects on the signal, such as propagation power loss and phase shifts, reflections from scattering, cross-talk, antenna coupling, and polarization. The entire MIMO channel can now succinctly be characterized by the linear algebraic relationship

$$\mathbf{Y} = \sqrt{\rho}\mathbf{H}\mathbf{C} + \mathbf{N}. \tag{1.2}$$

The information theoretic capacity of such a channel, i.e., the maximum theoretical supportable data rate is given by [2]

$$C = \log_2 det[\left(I + \frac{\rho}{t} H H^{\dagger}\right] \text{ bits/sec/Hz}. \tag{1.3}$$

It can be inferred from the above discussion that

1) the capacity of the MIMO channel grows approximately linear with the minimum of the number of transmit and receive antennas.

2) Exploitation of this scheme requires sophisticated coding and signal processing algorithms. Currently two avenues are pursued, namely Space-Time Layering(Lucent's Blast Project), and Space-Time Coding(AT&T Bell Labs).

1.3 Thesis Objective

The objective of this Thesis is to design antennas which can be used in the multiple-antenna system described above. The basic requirements are outlined below:

1) The antenna must be of low-profile or in other words it must be dimensionally small so that it can be incorporated in the portable mobile systems.

2) It has to be a novel design and must be of robust construction.

3) The design should be such that the information capacity is maximized for given geometric scenarios.

4) The simulational tool used should be able to characterize accurately the antenna performance. The tool used should also be able to simulate all the antenna parameters such as return loss and radiation pattern in all the planes of polarization with high degree of accuracy and should also be able to explore the various methods to further improve the antenna's performance.

Based of the above given requirements, it is seen that a novel microstrip antenna would be a very good choice as it has the advantages of low profile, low cost, robust construction, ease of fabrication and testing and suitability of incorporating into mobile sets. The simulational tool selected is the Finite Difference Time Domain technique and it is preferred over the other numerical techniques available.

System Overview

The high-level block diagram of the project is given below in fig.1.3. The other specifications involved are:
1) The Xilinx interface generates Rectangular chip waveforms, which has an approximate bandwidth of 1MHz.
2) The rectangular waveforms have peak-to-peak voltage of 2.5 to 3.3V and a chip rate 614.4 kchips/s.
3) RF modulation has to be used with or without IF intermediate to 900MHz. The above given set-up is used in the testbed to analyze the multiple-antenna system's

performance.

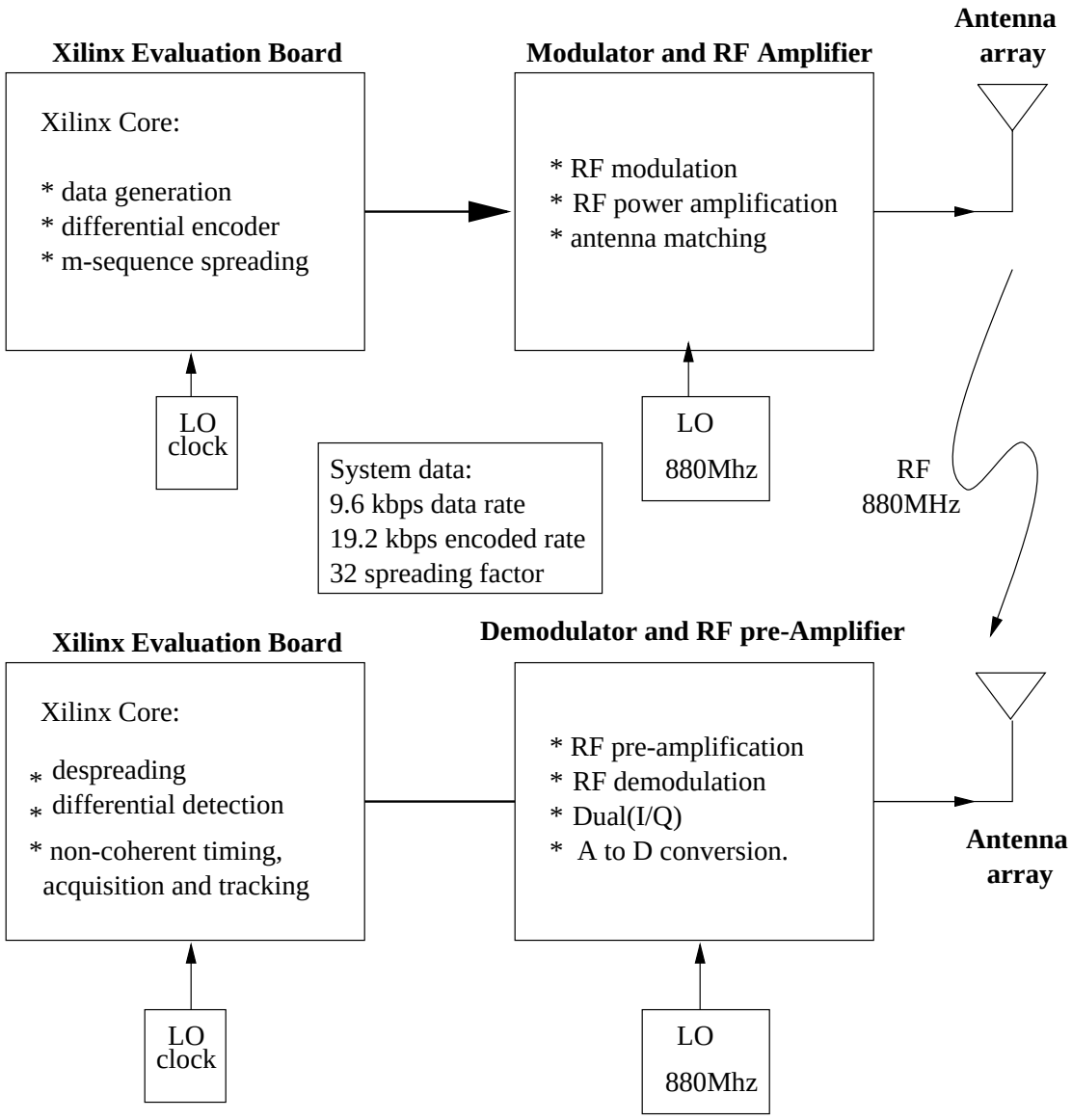

Figure 1.3: Hardware Testbed

1.4 Numerical Techniques in Electromagnetics

Numerical Techniques are exceptionally important in electromagnetics. In fact, only a few simple problems in electromagnetics can be solved analytically. For more

complex and real-life problems we have to use the numerical techniques, for the approximate solution of Maxwell's equations. Most of the techniques are based on some form of discretization, which implies that the integro-differential equations which characterize any given problem are solved by discretizing some of the variables in space, time or frequency. Some of the most popular and widely used techniques are listed below:

Methods of Moments(MOM)

This method is very popular and used extensively and it discretizes the integral-equation-solution forms of a given problem. This integral-solution approach is widely used in time-harmonic problems, for example, to calculate the radiating properties of antennas or scattering characteristics of dielectric and metal bodies. But this method involves the determination of the Green's function for the given structure, which can be quite tedious for a few types of geometry.

Finite Element Method(FE)

This method was initially used to solve problems pertaining to Civil engineering. This scheme exploits the fact that all systems work on the principle of least energy path. The concept of this method lies in discretizing the given structure into elements described by element-shape functions. These elements can be chosen as triangles, trapezoids or any suitable shape which helps in the discretizing process.

Finite Difference Time Domain method(FDTD)

The Finite Difference Time Domain method is one of the most popular techniques used for solving electromagnetic problems. It has been successfully applied to an extremely wide variety of problems, such as scattering from metal objects and dielectrics, design of antennas and to study the electromagnetic absorption by the human body exposed to radiation. The main reason of the success of the FDTD method resides in the fact that this method is extremely simple to formulate even for three-dimensional structures. This technique was first proposed by Yee and then later on improved by others including Allen Taflove[4] among others. Even now new

applications and additions are being realized which makes this method even more enticing. Therefore we choose FDTD to use as the numerical method to design the microstrip antennas.

Chapter 2

Finite Difference Time Domain method

2.1 Introduction

The basic theory behind solving electromagnetic problems using this method is to discretize Maxwell's equations both in time and space. This algorithm relies on the Yee's scheme which defines the spatial positions of the electric and magnetic field components which advance in time to simulate the time evolution of an Electromagnetic wave.

When Maxwell's equations in the differential form are examined, it can be seen that the time derivative of the E field is dependent on the Curl of the H field. This can be simplified to state that the change in the E field (the time derivative) is dependent on the spatial variation of the H field (the Curl). This results in the basic FDTD equation, where the new value of the E field is dependent on the old value(hence the difference in time) and the difference in the old value of the H field on either side of the E field point in space. Naturally this is a simplified description, which has omitted constants, parameters etc. The H field is found in the same manner. The new value of the H field at a given spatial position is dependent on the old value

(hence the difference in time), and the difference of the E field on either side of the H field point.

This description holds true for 1-d, 2-d, and 3-d FDTD techniques

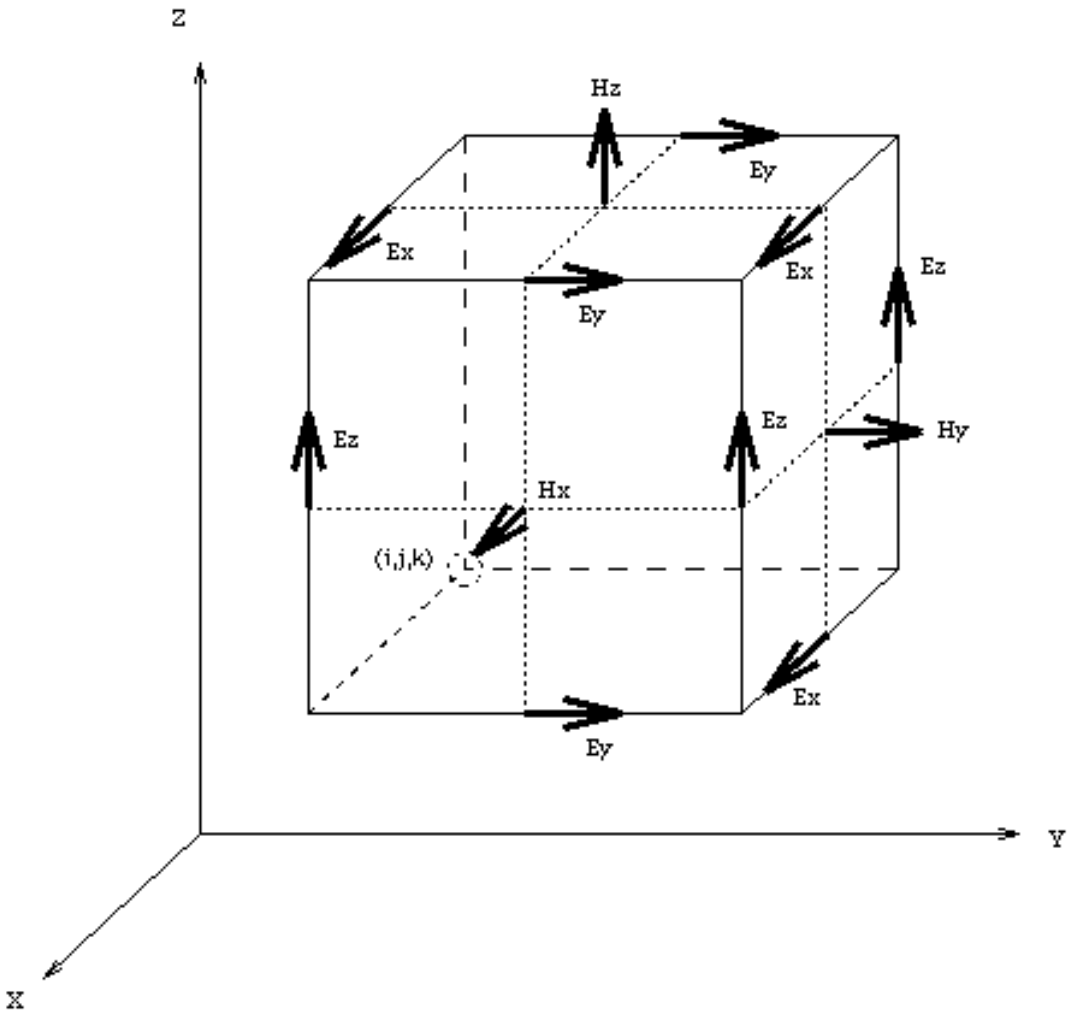

Figure 2.1: Standard Yee cell

2.2 FDTD Formulation

We know that the Maxwell's equations for a generic medium which may or may not contain dielectrics may be succinctly represented by the following two equations alone.

$$\frac{\partial E}{\partial t} = \frac{1}{\epsilon_0 \epsilon_r} (\bigtriangledown \times H) - \frac{\sigma}{\epsilon_0 \epsilon r} E \tag{2.1}$$

$$\frac{\partial H}{\partial t} = -\frac{1}{\mu_0} (\bigtriangledown \times E) \tag{2.2}$$

The antennas for the test-bed have been designed with a *D-H* formulation of the Finite-Difference Time-Domain method (FDTD) similar to that proposed in [5,6 and 7]. This formulation includes an effective implementation of the Perfectly Matched Layer (PML) boundary conditions that are completely independent to the background medium, and not involving from any real conductivity in the FDTD domain. The method involve adding fictitious dielectric constants and permeabilities ϵ_m and μ_m that are unrelated to the real values of ϵ_r used for specifying the materials in the FDTD space. The time domain equations for the six field components can be derived from the frequency domain expression of Maxwell's equations with fictitious dielectric constants and permeabilities to account for the PML materials. The D_z field component can be derived, for example, from the following normalized equation(2.3):

$$j\omega \left(1 + \frac{\sigma_x(x)}{j\omega\epsilon_0}\right) \left(1 + \frac{\sigma_y(y)}{j\omega\epsilon_0}\right) \left(1 + \frac{\sigma_z(z)}{j\omega\epsilon_0}\right)^{-1} D_z = c_0 \left(\frac{\partial H_y}{\partial x} - \frac{\partial H_x}{\partial y}\right) \tag{2.3}$$

where σ_m (m=x,y, or z) are fictitious conductivities. Equation (2.3) can be rewritten as

$$j\omega \left(1 + \frac{\sigma_x(x)}{j\omega\epsilon_0}\right) \left(1 + \frac{\sigma_y(y)}{j\omega\epsilon_0}\right) D_z = c_0 \left(\frac{\partial H_y}{\partial x} - \frac{\partial H_x}{\partial y}\right) \left(1 + \frac{\sigma_z(z)}{j\omega\epsilon_0}\right) \tag{2.4}$$

that, in time domain finite-difference formulation, results in the following explicit expressions:

$$curl_H = H_y^{n-1/2}(i+1/2,j,k+1/2) - H_y^{n-1/2}(i-1/2,j,k+1/2) + \\ + H_x^{n-1/2}(i,j-1/2,k+1/2) - H_x^{n-1/2}(i,j+1/2,k+1/2) \tag{2.5}$$

$$I_{Dz}^n(i,j,k+1/2) = I_{Dz}^{n-1}(i,j,k+1/2) + curl_H \tag{2.6}$$

$$D_z^n(i,j,k+1/2) = gi3(i)gj3(j)D_z^{n-1}(i,j,k+1/2) + \\ + gi2(i)gj2(j)0.5(curl_H + gk1(k)I_{Dz}^n(i,j,k+1/2)) \tag{2.7}$$

where the coefficients g are defined by:

$$gk1(k) = xn(k) \tag{2.8}$$

$$gi2(i) = 1/(1+xn(i)) \tag{2.9}$$

$$gj2(j) = 1/(1+xn(j)) \tag{2.10}$$

$$gi3(i) = (1-xn(i))/(1+xn(i)) \tag{2.11}$$

$$gj3(j) = (1-xn(j))/(1+xn(j)) \tag{2.12}$$

The coefficient xn is used to describe the profile of the Perfectly Matched layers(PML). The PML is used as the boundary of the computational space in order to simulate free space. These layers having fictitious electric and magnetic conductivities absorb the incident EM fields with almost no reflections thereby simulating a free space. The PML formulation is found to give lower reflections compared to the other methods, such as, Retarded-time method and Mur's method [8] among others.

Similar equations can be derived for all the other field components of the D field, namely x and y components. The E field can be derived directly from the D field. The E field at all the points in the total grid is to be known in order to calculate the corresponding H field, which in turn is required to determine the D field for the next time step. Therefore this scheme has a time-step marching or what is popularly

called a "leap-frog" scheme. The discretized equation determining the E_z field is given below (2.13).

$$E_z^n(i,j,k) = gaz(i,j,k)(D_z^n(i,j,k) - I_z^{n-1}(i,j,k)) \tag{2.13}$$

where I_z is given by the equation:

$$I_z^n(i,j,k) = I_z^{n-1}(i,j,k) + gbz(i,j,k)E_z^n(i,j,k) \tag{2.14}$$

and the coefficients gaz and gbz are given as follows:

$$gaz(i,j,k) = 1/(\epsilon_r + (\sigma \times dt/\epsilon_0)) \tag{2.15}$$

$$gbz(i,j,k) = \sigma \times dt/\epsilon_0 \tag{2.16}$$

The equations determining E field components in x and y directions can also be similarly derived.

Discretizing the other Maxwell equation we arrive at the following space-time iterative equation for H field. Given below is the equation for Hx field (2.17).

$$\begin{aligned} H_x^n(i,j,k) &= fj3(j)fk3(k)H_x^{n-1}(i,j,k) + \\ &+ fj2(j)fk2(k)12(curl_E + fi1(i)I_{hx}^n(i,j,k)) \end{aligned} \tag{2.17}$$

where $curl_E$ and I_{hx} are given by:

$$curl_E = (E_y^n(i,j,k+1) - E_y^n(i,j,k) - E_z^n(i,j+1,k) + E_z^n(i,j,k)) \tag{2.18}$$

$$I_{hx}^n(i,j,k) = I_{hx}^{n-1}(i,j,k) + fi0(i)Curl_E \tag{2.19}$$

and the coefficients f are defined as:

$$fj2(j) = 1/(1 + xn(j)) \tag{2.20}$$

$$fj3(j) = (1 - xn(j))/(1 + xn(j)) \tag{2.21}$$

$$fk2(k) = 1/(1 + xn(k)) \tag{2.22}$$

$$fk3(k) = (1 - xn(k))/(1 + xn(k)) \tag{2.23}$$

$$fi0(i) = 1 \tag{2.24}$$

With this FDTD code, microstrip patch antennas have been designed to operate with the wireless smart antenna test-bed, and the selected frequency of operation has been centered around 880MHz.

The microstrip antenna's physical characteristics are incorporated in the three-dimensional FDTD grid by specifying the material in each cell of the grid with a dielectric constant ϵ_r and conductivity σ. These values of the dielectric constant and conductivity is included in gaz, gbz and other coefficients and in effect change the flow of EM fields through each cell, controlled by the governing equations described above, thereby simulating precisely the field-distribution in the entire grid. Current and Voltage, if necessary can then be calculated at any point in the grid by the curl of H field and line integral of E field respectively. The voltage and current can be found for the source 'cell' and a Fourier transform performed on them would yield the frequency domain values of voltage and current , which in turn can be used to find the frequency domain impedance, reflection coefficient and voltage standing wave ratio. These values can give an insight into the performance of the antenna system. The FDTD code also enables us to determine numerically the radiation patterns for any antenna.

Chapter 3

Microstrip Antenna Design

3.1 Introduction

3.1.1 Definition of Microstrip Antenna

A microstrip antenna in its simplest form consists of a radiating patch on one side of a dielectric substrate , and has a ground plane on the other side. The patch or top layer can be of any shape, but conventional shapes are generally used to simplify analysis and performance prediction. Ideally the dielectric constant ϵ_r should be low, so as to enhance the fringe fields which account for radiation. However, other performance and design requirements may dictate the use of substrates whose realistic dielectric constants may be greater than, say 5. Various types of substrates having a large range of dielectric constants and loss tangents have been developed.

3.1.2 Advantages and Disadvantages of Microstrip Antennas

Microstrip antennas have several advantages compared to the conventional antennas and therefore are used in many applications over a frequency range from approximately 100MHz to about 50GHz and higher.

The main advantages are:

1) Lightweight, low volume, low profile planar configurations are possible.

2) Low fabrication cost and ease of fabrication.

3) The antennas have low scattering cross section.

4) Linear and Circular polarizations are possible with simple changes in the feed position.

5) Dual frequency operation can be attained easily and cavity backing is not a necessity.

6) Feed lines and matching networks are simultaneously fabricated along with the antenna structure.

7) They are compatible with modular designs(solid state devices such as oscillators, amplifiers, variable attenuators, switches, modulators, mixers, phase shifters etc can be added directly to the antenna board).

However, microstrip antennas also have some short-comings compared to conventional microwave antennas including:

1) Narrow bandwidth.

2) They are lossy and therefore have somewhat lower gain.

3) Most of the conventional microwave antennas radiate most of the energy into only a half plane.

4) Relatively poor end-fire radiation performance.

5) Poor isolation between the feed and the radiating elements.

6) Possibility of excitation of surface waves.

It is possible, however, to find remedy of some of these disadvantages by using appropriate designs. The narrow bandwidth and lossy nature are inherent to the microstrip structure but the other listed disadvantages can be rectified thus:

1) Though as an element these antenna radiates only in one half plane but when used as an array, the array factor comes into play , which can be manipulated by means signal-processing algorithms enabling dynamic beam shaping and beam steering.

2) By carefully designing an array, it is possible to quantify the impact of coupling between the elements and ways can be found to minimize coupling effect, and give greater isolation between array elements.

3) The big impediment namely, the excitation of surface waves can be minimized by using a new technique which employs "High Impedance Ground Plane" or what is otherwise called a Photonic bandgap substrate. This issue is analyzed in greater detail in chapter5.

3.1.3 Radiation Mechanism of a Microstrip Antenna

Radiation from microstrip antennas can be described by considering the simple case of a regular rectangular microstrip patch, placed a small fraction of wavelength above the flat conducting ground plane, as shown in figure 3.1. If we assume that there are no variations of the electric field along the width and the thickness of the microstrip structure, the electric field configuration of the radiator along the length is shown in figure 3.2. The field vary along the patch length which is approximately half the wavelength ($\lambda/2$) in conventional microstrip patches. Radiation can be mostly ascribed to the fringing fields at the open circuited edges of the radiator. If the fringing fields are resolved into its parallel and tangential components with respect to the ground plane, the normal components would be out of phase with each other and therefore would cancel out each other. In other words the normal components does not contribute to the far field radiation. The tangential components are in phase and the resulting tangential field components combine to give maximum radiated field normal to the surface of the patch, that is , the broadside direction. Therefore, the patch may be represented by two slots $\lambda/2$ apart excited in phase and radiating in the half space above the ground plane.

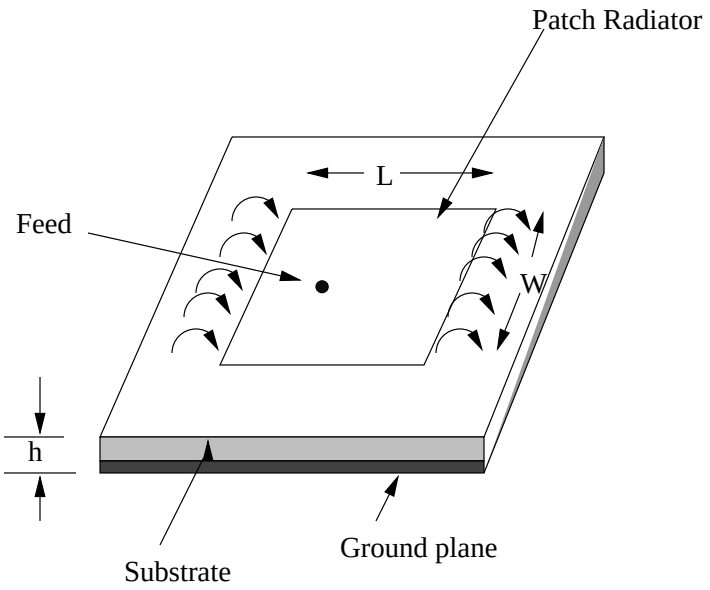

Figure 3.1: Rectangular patch antenna.

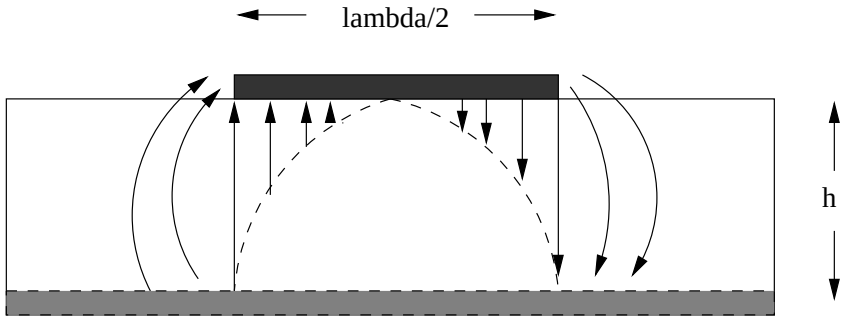

Figure 3.2: Side view of the microstrip antenna.

3.2 Design of Electrically-Small Microstrip Antenna

3.2.1 Introduction

As seen from the theory given above, the regular rectangular patch has a length of half the effective wavelength ($\lambda/2$) corresponding to the frequency of operation. When operating at frequencies such as 880MHz, it is seen we would require an antenna approximately 17cm long when the substrate is air, which is not practical for use in the modern communication systems. Therefore it is necessary to reduce the size of the patch-radiator substantially and still make it perform at the same frequency of operation. The first stage of reduction of size is achieved with the dielectric substrate. We know that the speed of an EM wave traveling through a dielectric substrate is slower, or in other words the wavelength of the EM wave reduces by a factor of $\sqrt{\epsilon_{eff}}$, where ϵ_{eff} depends on ϵ_r of the substrate, the height and width of the substrate and the ϵ_r of air(which is 1). The substrate we use in the new patch design has a dielectric strength of 3.05. But this reduction may not be enough to achieve any realistic real-estate saving. Therefore, additional design techniques have to be employed to achieve the reduction in size of the microstrip patch and also of the ground plane.

3.2.2 Shorted-pin Microstrip Antenna Design

The conventional shorted microstrip antenna is constructed by short-circuiting the entire width of the zero potential plane of a regular antenna, or what is popularly called a Quarter wavelength antenna. We can construct a partially shorted microstrip antenna, by shorting only a portion or few portions of the zero potential plane. The total width of the shorted sections controls the resonant frequency and the input impedance of the shorted microstrip antenna. Reducing the width of the shorted edge, proportionally increases the loading inductance of the antenna and hence, decreases the resonant frequency. As fabricating short circuit portions in these kind of partially shorted antennas is a relatively difficult task, shorting pins are generally used. The

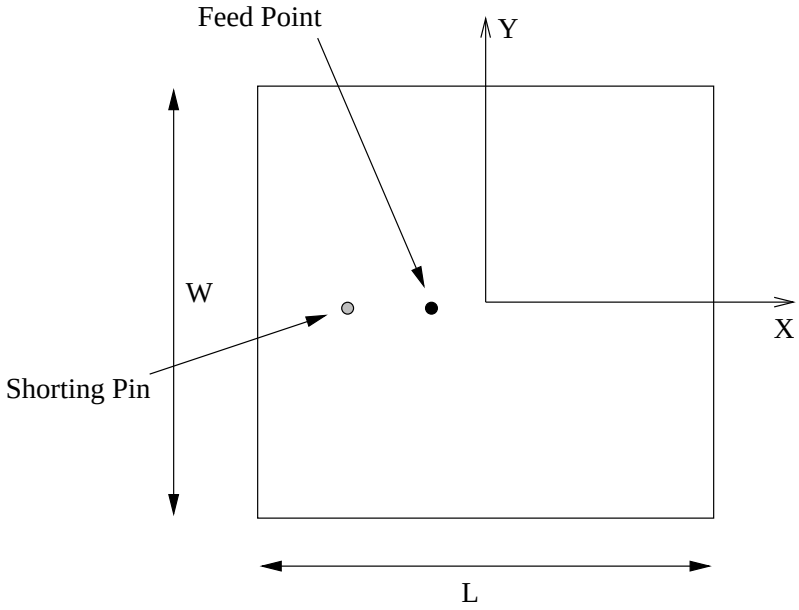

Figure 3.3: An example single-shorting pin patch.

antennas made by using shorting pins have been experimentally and numerically studied. As shown in [9,10,11,12 and 13], the maximum reduction in physical size can be achieved if a single shorting post is used. The patch dimensions are reduced by a factor of three or four, making the antenna size well suited for portable handsets. An example of such a structure is shown in fig(3.3).

The shorting pin located close to the feed point results in a significant reduction in overall patch size. The principle behind this can be easily explained in terms of simple circuit theory. The typical RLC circuit used to describe a probe fed patch is loaded with a parallel LC circuit. The shorting pin effect on the input impedance of the antenna can be represented by the LC combination. When the shorting pin is located near the feeding pin, a strong capacitive coupling or loading is produced. This results in cancelling the inductive nature of a patch below resonance. Therefore the amount of capacitive loading induced determines the ultimate reduction in size. As the shorting pin is moved away from the feed, the capacitive coupling decreases and inductive reactance increases, very similar in form to that typically used to represent the effect of the feed itself. Thus at a fixed frequency, the shorted patch size can be

increased or decreased, depending on the distance of the pin from the feed. Therefore for a single shorting pin antenna, accuracies of a fraction of a millimeter are required for close positioning between the feed and the shorting pin. The other most significant drawback of this shorted pin microstrip antenna is the relatively high cross polarized fields generated.

The close proximity of the feed and shorting pins in antennas operating at relatively lower frequencies like 800-900MHz, can make the fabrication process difficult. Therefore the issue of improving the manufacturing ease of a shorted patch is addressed and a simple technique is used. As suggested in [9,10 and 13],development of a stronger shorting plane results in an an improved matching and an increased bandwidth. There are two methods by which a stronger shorting plane can be developed. One method is to increase the thickness of the shorting pin and the other is to increase the number of shorting pins employed. Following the latter, we employ two shorting pins located near the feed point in this design. To get maximum reduction, the shorting pins have to be placed very close to the patch edge. We know from the above discussion that in order to reduce the inductive loading the shorting pins have to be close to the feed. It has to be observed that many different positions of the feed and shorting pins are possible and a fair degree of freedom exists in this kind of a design. The better antenna performance is, however achieved at the expense of a larger patch area compared to a single shorting-pin patch design, but its merits outweighs the disadvantages and therefore this design is followed.

3.2.3 The New Microstrip Antenna with Dual Shorting Pins

This antenna was designed with the following requirements in mind.

1) This antenna should be of smallest dimension possible.

2) As reduction in patch area subsequently results in decrease in bandwidth and gain, which are two of the important antenna characteristics, therefore there is a trade-off.

3) The return loss should be minimal.

4) A radiation pattern without prominent nulls in the radiating plane of the antenna

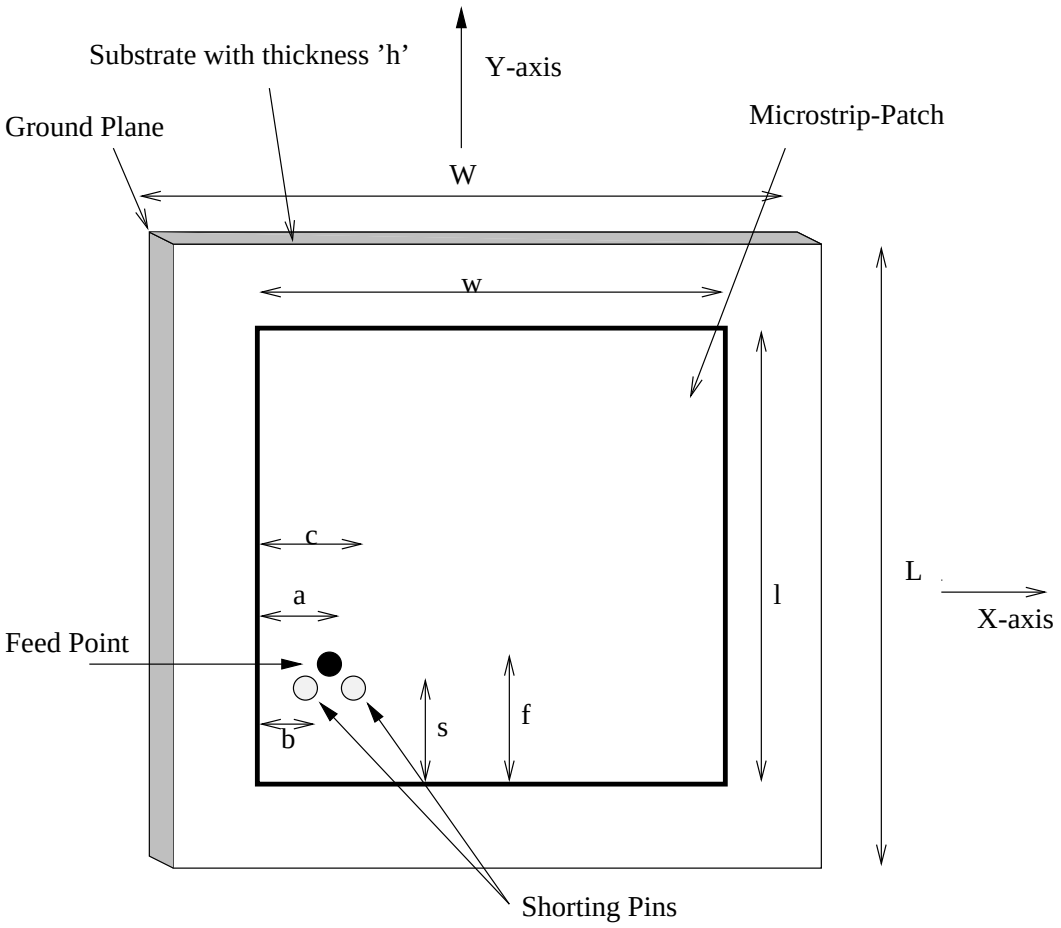

Figure 3.4: Dual Shorting pin microstrip antenna.

should be achieved.

With the above given constraints an antenna was designed and simulated using FDTD method and the schematic of it is given in fig 3.4.

The dimensions given in the schematic are as follows: l= 28.5mm, w= 34.75mm, a= 3mm, b= 2mm, c= 4mm, f= 7.5mm, s= 6mm, h= 1.5mm, L= 48.5mm, W= 54.5mm.

FDTD specifications used for this design:

The Grid resolution used is 0.5 mm^3. Other values for resolution were also applied to verify the correctness of the results obtained.

The total FDTD space used is $140 \times 140 \times 40$ cells in the x, y, and z directions, respectively. Out of these 12 layers have been used to describe the PML boundary layers in order to ensure sufficient absorbing characteristics of the boundary. The remaining space is used to specify the entire antenna structure.
A gaussian pulse, applied with a resistive source [14], has been used as a source. This resistive source reduces the simulation time without compromising on the accuracy of the results.
20,000 time steps were required to attain convergence of simulation. Proper convergence of the simulation is critical for the accuracy of the results.

Fabrication and Experimental results

The antenna designed and simulated computationally is fabricated and tested to verify its correct operation. The fabrication was carried out by milling the required rectangular shape on the microwave laminate. Holes were drilled to connect the 50Ohm SMA coaxial connector and also to lodge the shorting pins in the structure. A network analyzer, model.8510, was used to measure the S11 or return loss of this antenna, which is plotted in figure 3.6. As shown, the simulated and experimental results agree well. The -10dB bandwidth, which corresponds to a VSWR valus of 2, is found to be 9MHz and the -3dB bandwidth, which corresponds to a VSWR value of 3, is found to be 20MHz. . This relatively narrow bandwidth results due to many factors, including use of shorting pins and a thin substrate with a low value of dielectric constant. All these factors assist in reducing the size of the patch but at the expense of bandwidth and gain. However this bandwidth of 8MHz is sufficient for the multiple-antenna testbed being tested. The normalized radiation patterns in all planes have been simulated. The maximum gain of the radiation pattern is found to be approximately -8dbi.

As seen there is a non-negligible radiation towards the side below the ground plane, mainly due to the small ground plane used. This may have some advantages in a few applications where a near-isotropic radiation pattern is required or in cases where a high sensitivity to cross polarizated field is required. This may be also used

when there is severe constraint on the antenna real estate . However, some other applications may require a bigger ground plane. The E field in theta direction along the X-Z plane is plotted for different ground plane sizes in figure(3.7) and (3.8). As shown, the larger ground plane with a length of 53.5mm and a width of 59.5mm, reduces the back-radiation and also improves the directivity in the front-side.

Performance of Dual shorting pin Microstrip Antenna with respect to a regular half wavelength microstrip Antenna

In order to evaluate the relative performance of the dual shorting pin antenna with respect to a regular half wavelength antenna, a half wavelength antenna is also simulated, fabricated and tested and a comparative study of each of these two antennas is conducted. As the substrate used has a dielectric constant of 3.05, the length of the patch radiator is approximately half of the guide wavelength for this regular half wavelength antenna, where guide wavelength depends on the dielectric constant of the substrate. The FDTD specifications used for this non-shorted regular antenna are as follows. The Grid resolution used is 0.75 mm^3. The total FDTD space used is $219 \times 138 \times 50$ cells in the x, y, and z directions, respectively. 10 layers have been used to describe the PML boundary layers.

In this case too a gaussian pulse, applied with a resistive source [14], has been used as a source to determine the return loss in a frequency range. 30,000 time steps were required to attain convergence of this simulation.

This antenna is fabricated and measurements were recorded. The regular half wavelength microstrip antenna is found to have a -10dB bandwidth of 13.5 MHz and a -3dB bandwidth of 26 MHz. The maximum gain of the radiation pattern was found to 1 dBi. It is therefore seen that the reduction in size results in reduction in bandwidth and gain as well. Therefore it is realized that the use of electrically smaller antennas like the one designed above always involves trade-off issues, as reduction in size must be achieved at the expense of bandwidth and gain.

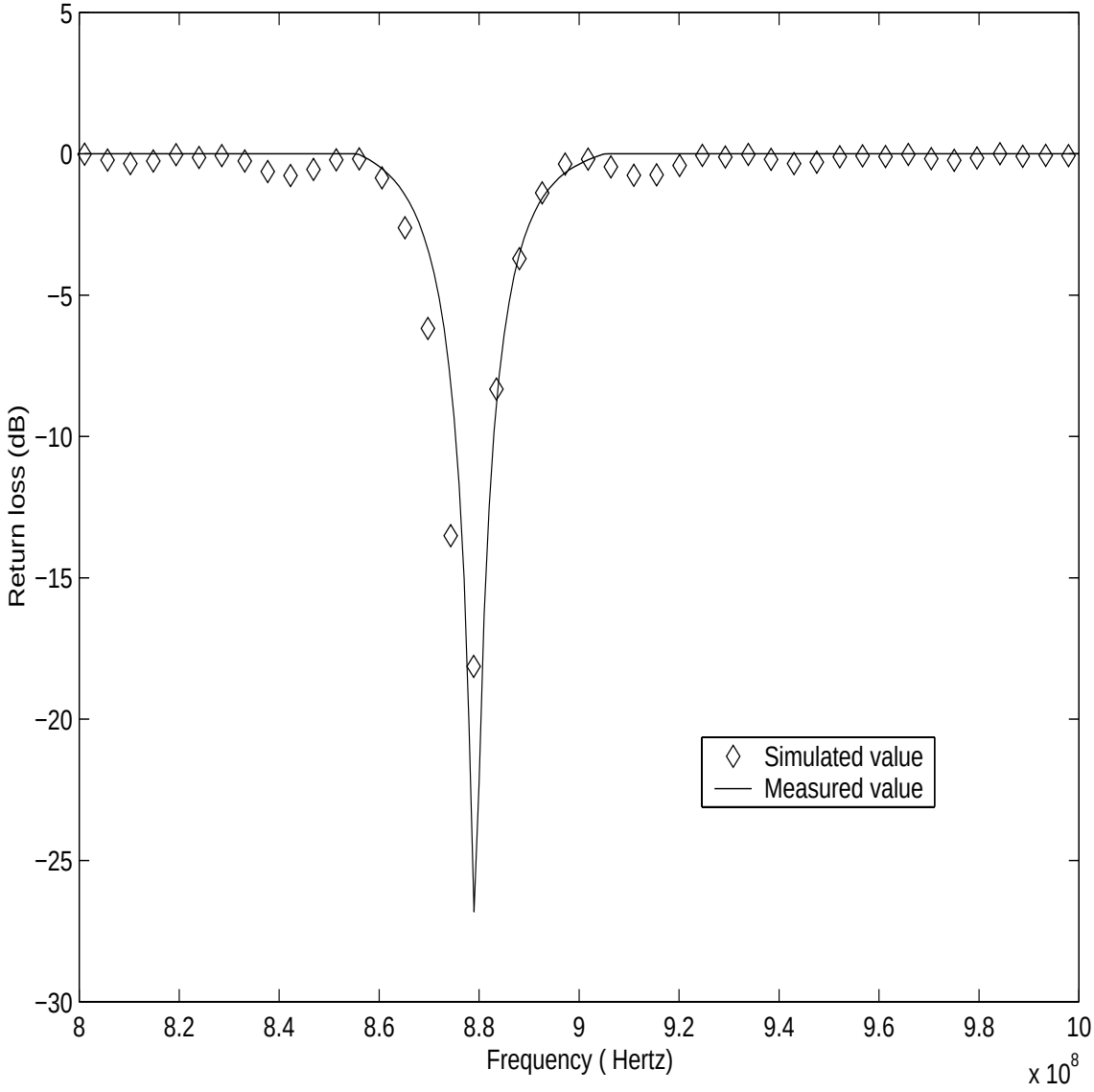

Figure 3.5: Return loss of the Dual-Shorted Pin Antenna.

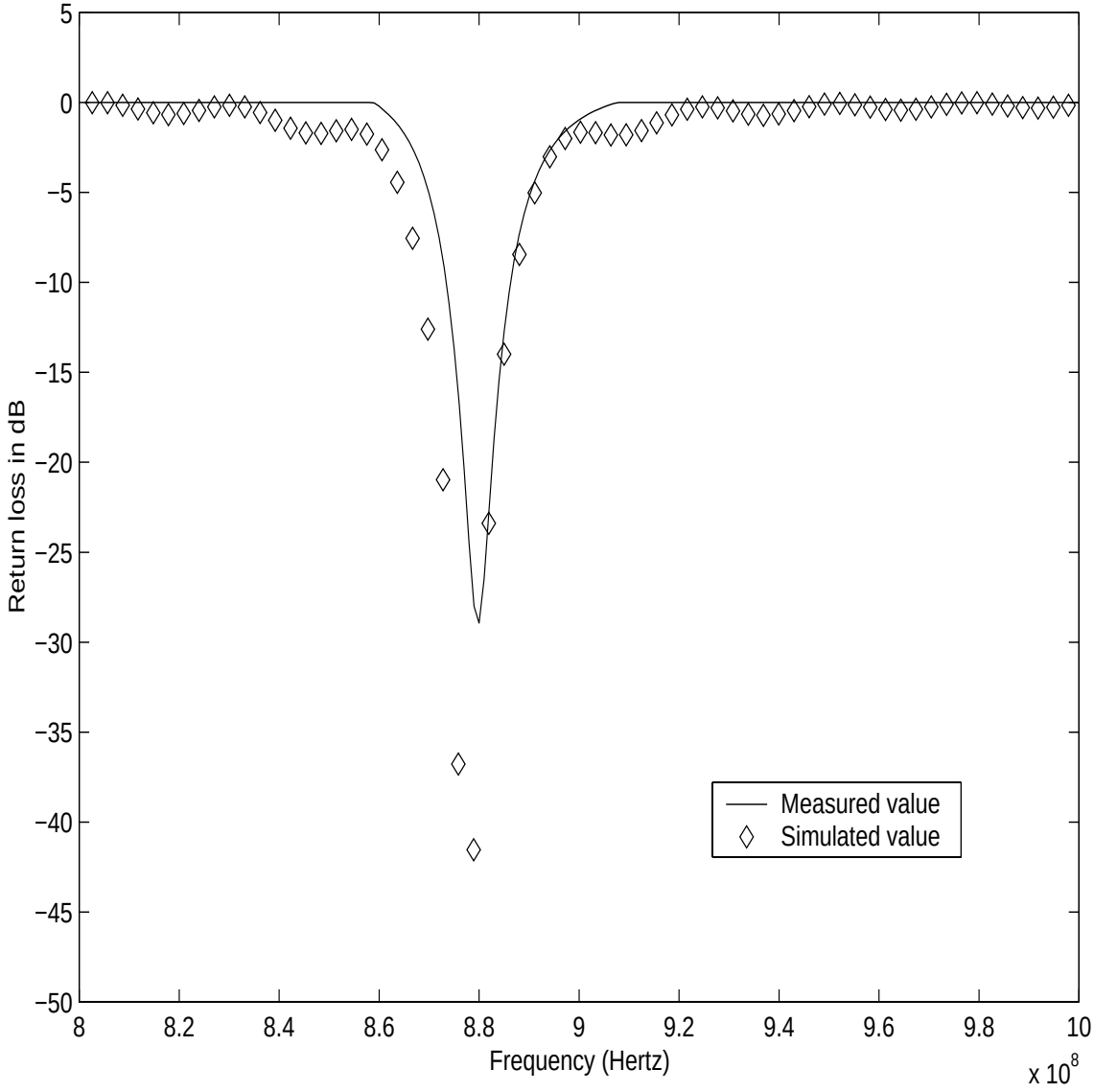

Figure 3.6: Return loss of the regular half wavelength microstrip Antenna.

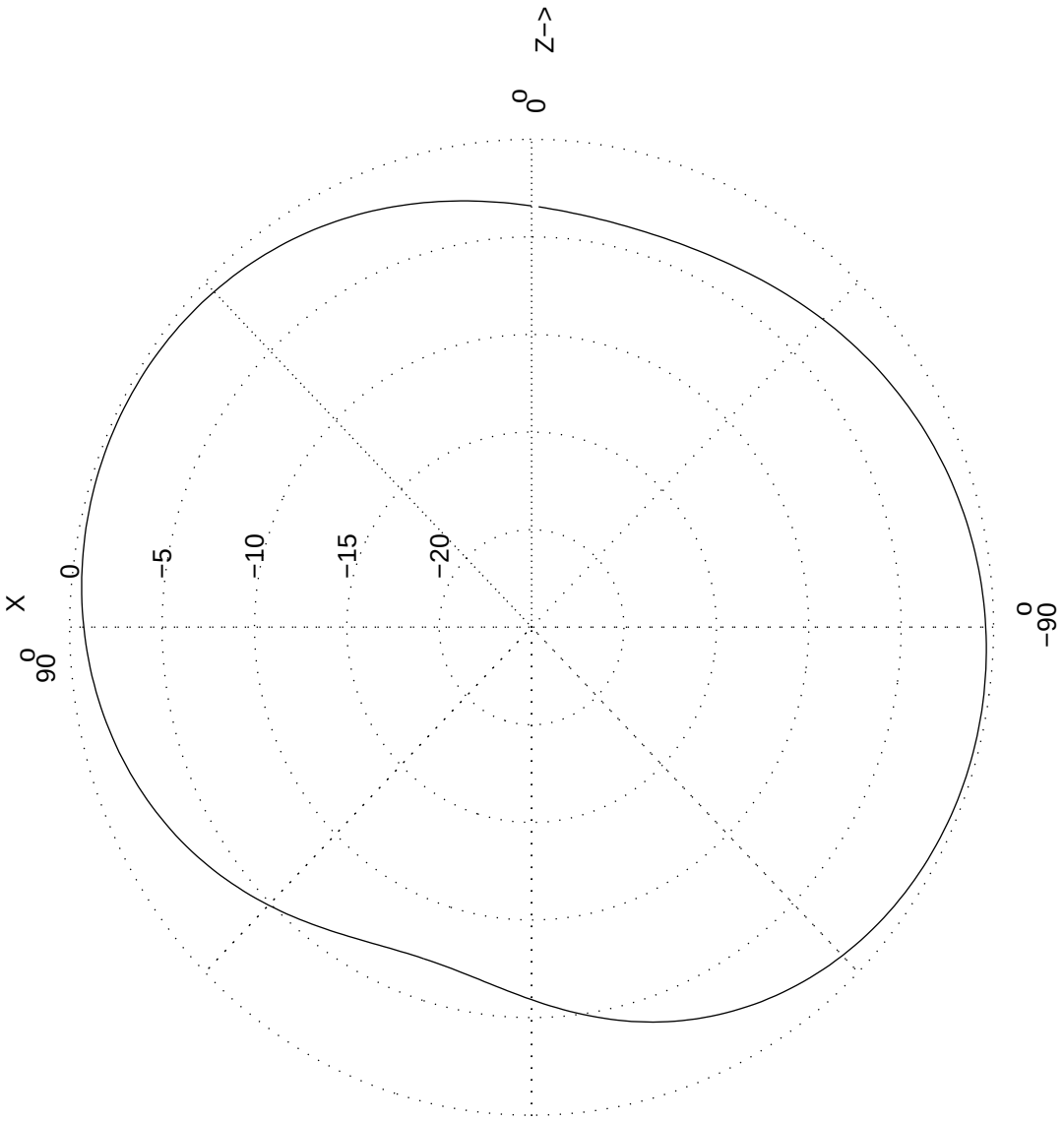

Figure 3.7: Normalized E field in theta direction and in XZ plane for the dual shorting pin antenna.

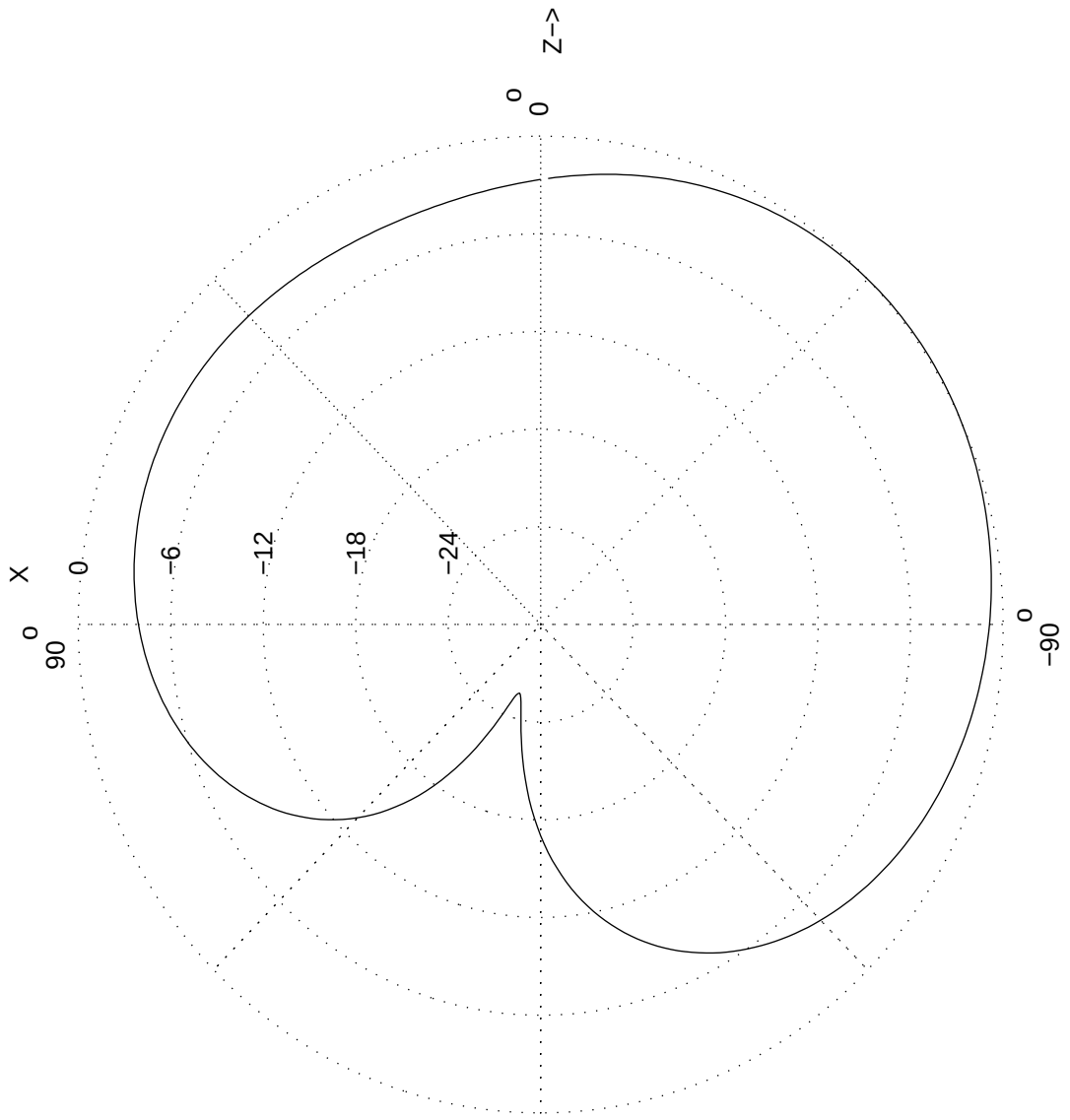

Figure 3.8: Normalized E field in theta direction and in XZ plane for a bigger ground plane for the dual shorting pin antenna.

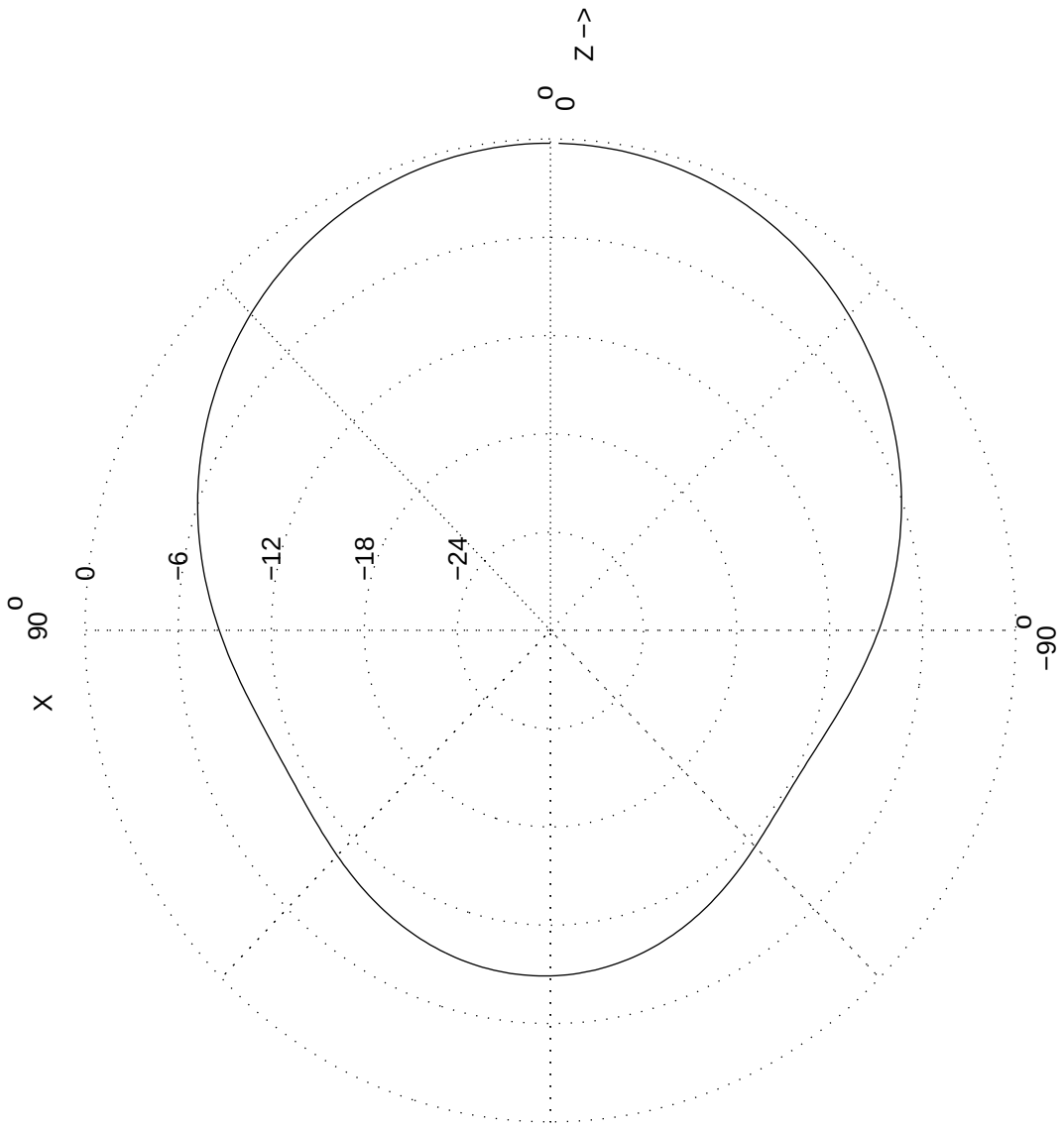

Figure 3.9: Normalized E field in theta direction and in XZ plane for the regular half wavelength antenna.

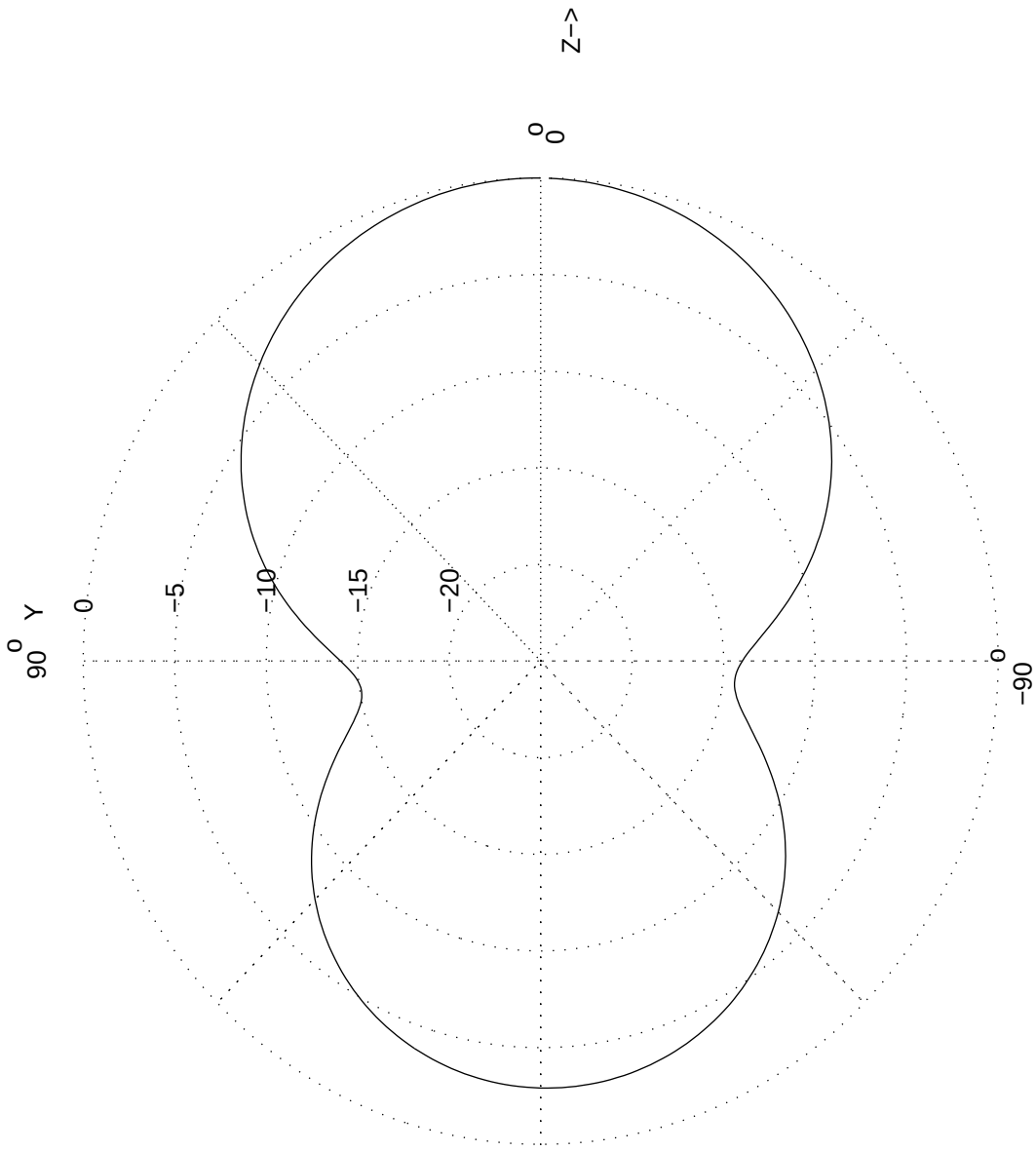

Figure 3.10: Normalized E field in phi direction and in YZ plane for the dual shorting pin antenna.

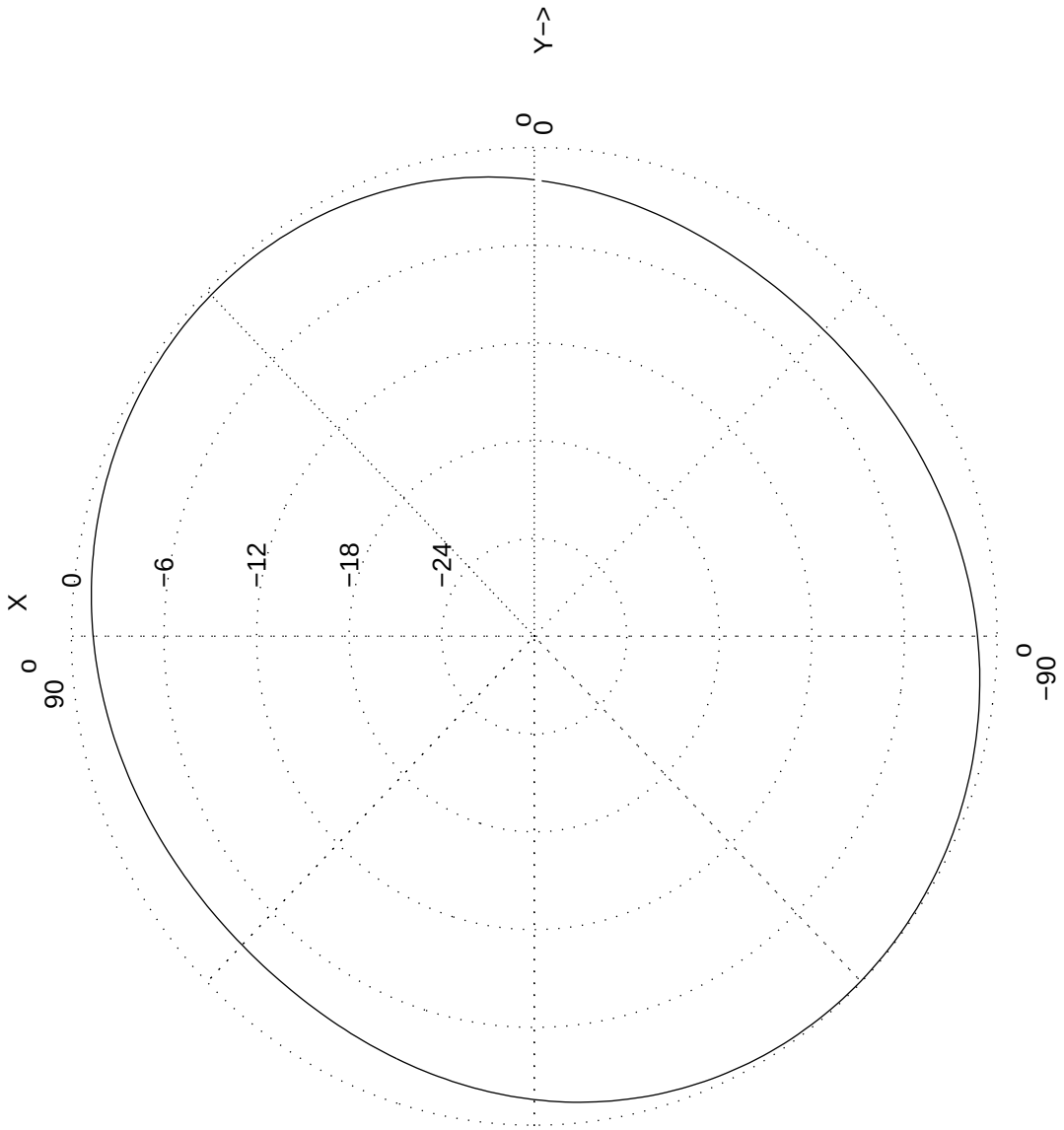

Figure 3.11: Normalized E field in theta direction and in XY plane for the dual shorting pin antenna.

Chapter 4

RF Design for the Testbed

A RF circuit is designed to convert the digital signals to analog frequencies centered around 880MHz, which are then transmitted using the antenna over the channel to be retrieved at the receiving end. This design assumes that this test will be run with short distance(less than 3 m) between transmitter and receiver.

4.1 Transmitter draft

I and Q signals are generated by the Xilinx interface, and they are fed as inputs to the transmitter. The different components of the transmitter is described below:

Attenuator

An attenuator is required as the high voltage signals of 2.5vpk cannot be fed directly to the modulator, as it may damage the modulator and therefore we need to reduce the voltage levels of the inputs. A Resistive attenuator is used and it decreases the volatge level of 2.5vpk to 178mvpk. The attenuator should also be matched on both sides to an impedance of 50Ohms.

The design equations involved to determine the component values in the given

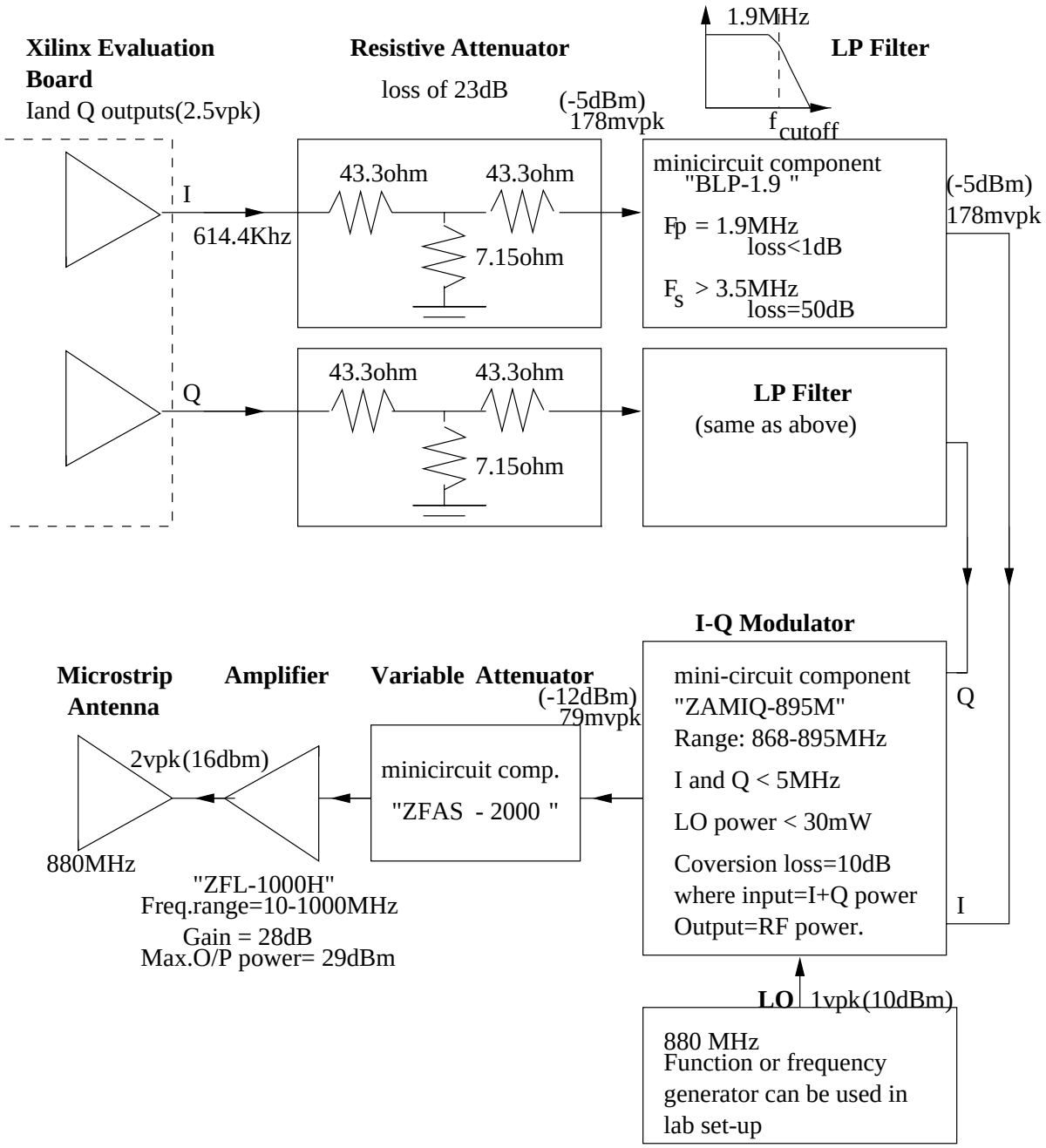

Figure 4.1: Transmitter Draft

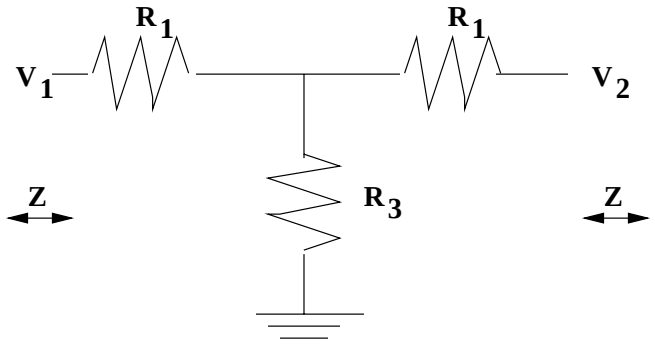

Figure 4.2: Resistive Attenuator

resistive attenuator , shown in 4.2 are:

impedance looking into both sides, $Z = 50ohms$

k is the transformation ratio and is determined thus:

$K = 2500/178$

The equations determining the values of R_3 and R_1 are:

$R_3 = 2Z/(K - 1/K) = 7.15ohm$

$R_1 = Z(1 - 2/(K + 1)) = 43.3ohm$

When these resistor values are used in this circuit, it provides the required attenuation.

Low Pass Filter

The minicircuit(vendor) component BLP-1.9 has been used to implement this. This component filters low frequency stray signals and noise. The output of the filter has a magnitude of 178mVpk(-5dBm), and which is in turn fed to the I-Q modulator. The filter is found to give no attenuation in the pass band.

I-Q Modulator

The minicircuit component ZAMIQ-895M has been used for this purpose. This component is fed with the I and Q signals each of which have a power of -5dBm and

the local oscillator signal with an amplitude of 1Vpk(10dBm). The conversion loss of the modulator is 10dB. The output is an RF signal at 80mVpk(-12dBm).

Transmitter Amplifier

The modulated signal is then amplified using an amplifier. The component used for this purpose is minicircuit's ZFL-1000H, which gives an amplification of 28dB and as a result, the signal at the antenna terminals is found to be 2VpK(16dB).

Variable Attenuator

A variable attenuator namely minicircuit's ZFAS-2000 has been used. This component is used to adjust and achieve the correct power levels at the transmitting antenna terminals.

4.2 Receiver Draft

It is noted that the received signal has a power of -20 to -30 dBm which corresponds to 32mVpk in voltage magnitude. The transmission of the signals is through air, which accounts for the loss of power of the signals.

Receiving Amplifier

The -20dBm signal which the antenna approximately picks up, is fed directly to the amplifier. The amplifier gives sufficient amplification before feeding the signals as inputs to the I-Q Demodulator. As it is known that the very first stage of any receiver system needs to be a Low-noise amplifier as the receiving antenna may pick up a contaminated, noisy signal, we select a Low noise amplifier which also provides the requisite amplification. The minicircuit component ZEL-0812LN , which has a gain of 20dB, is selected for this purpose. The output of this component is a signal at 0dBm or 317mVpk, which again, asts as the input to the demodulator.

I-Q Demodulator

This component demodulates the incoming signal back to I and Q components. .

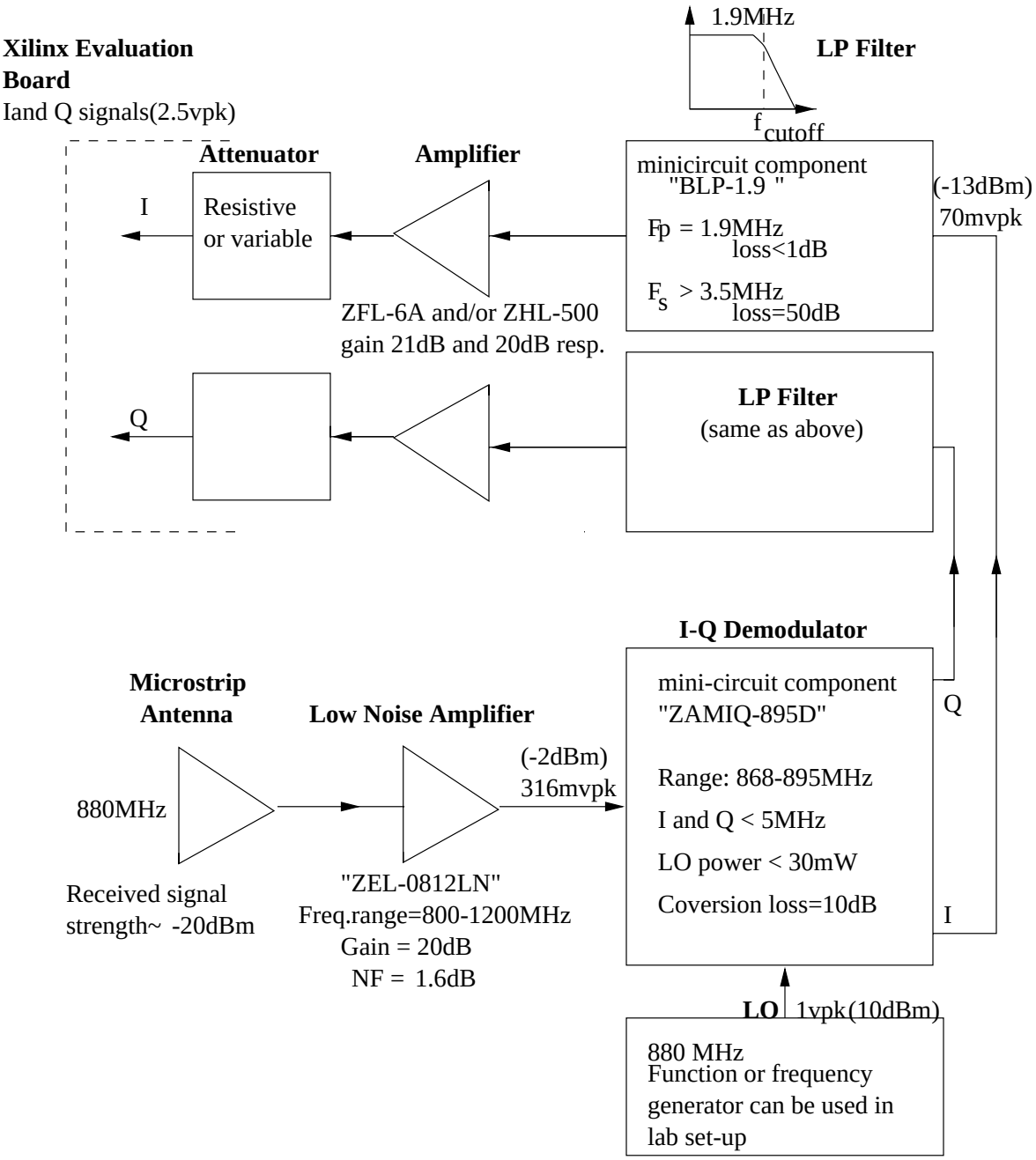

Figure 4.3: Receiver Draft

Along with the reproduced I and Q signals , the output of the demodulator also contains the intermodulation products and some stray or noise signals and therefore the useful I and Q signals need to be filtered out using a Low-Pass filter. The component used for the demodulator is ZAMIQ-895D.

Low Pass Filter

The component BLP-1.9, which is used in the transmitter can be used to reproduce the I,Q signals at the receiving end too. The output of the filter has to be amplified to raise it up to the requisite levels in order to detect them.

Amplifiers

As the I and Q signals has to be raised to the requisite levels , amplifier have to be used. We have used two amplifiers in this case, in cascade if required to get the required signal levels. The components used are ZFL-500 and ZHL-6A. Here a resistive attenuator or a variable attenuator can to be used if needed to get the signal upto the right level.

Chapter 5

Future Work

5.1 High Impedance Ground plane

Some prominent shortcomings of the proposed antenna are that, the bandwidth is relatively narrow, a common problem in all the shorted-pin patch antennas, and the E-field radiation pattern indicates significant radiation behind the ground plane. In addition to that, all microstrip antennas are lossy due to a generation of surface currents. Therefore, ways are investigated which can improve the performance of the antenna.

Recently a new kind of ground plane has been developed that is capable of suppressing the propagation of radio frequency surface currents. This surface is important for antenna applications, because it has the property of partially isolating the radiating elements from the nearby electromagnetic surroundings. This surface also provides a high electromagnetic surface impedance for a particular band of frequencies determined by its geometry, which can help increase the radiation from the patch in the front side and also decrease the radiation escaping into the backside in that frequency band. The bandwidth of the antenna, as a result, is also improved.

The high impedance electromagnetic surface is made of continuous metal. It

Figure 5.1: High Impedance ground plane with one layer of resonant elements.

Figure 5.2: High Impedance ground plane with two layers of resonant elements.

conducts DC currents, but does not conduct AC currents within a forbidden frequency band[15,16 and 17]. The physical geometry consists of a metal sheet, textured with one or two layers of two-dimensional lattice of resonant elements, which acts as a two-dimensional filter to prevent the propagation of electric currents.

The high-impedance properties occur near the resonance frequency of the surface, $\omega = 1/\sqrt{LC}$, where L is the effective sheet inductance and C is the effective sheet capacitance. In the surface with a single layer of resonant elements as shown in fig 5.1, the capacitance is caused due the separation between the adjacent elements, and the capacitance achieved by this layout is quite less and therefore the frequency ω would be high. For lower frequencies such as the PCS bands the second scheme would have to be used given in fig 5.2, as here the capacitive effect is produced due to the elements placed parallel to each other and the separation between then is filled with a dielectric with dielectric strength ϵ_{r1}. The capacitance produced by this scheme is more than the single layer scheme and therefore is suitable for frequencies in and around PCS bands. The inductance of the surface is related to the thickness of the circuit board given by the equation $L = \mu t$. However, to operate this surface at frequencies such as 800-900 MHz range, we would require an even higher capacitance and therefore the separation between the two layers of resonant elements should be extremely less, which makes the simulation task relatively difficult.

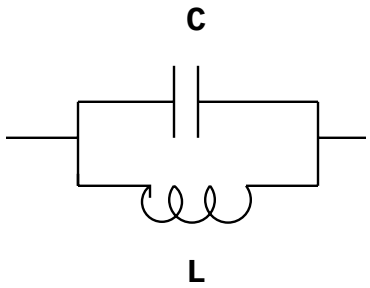

Figure 5.3: Equivalent circuit model for the high-impedance surface.

5.2 Characterization of MIMO wireless channels

Recent research on MIMO (Multiple Input Multiple Output) space-time channel has shown that high theoritical channel capacity can be achieved by using multiple antennas at the tramsmit and receive ends. This comes from the analysis which infers that the channel capacity is directly related to minimum number of transmit or receive antennas. The implementation of the V-blast[18] detection scheme in the lab-setup, has demonstrated spectral efficiencies of 20-40 bps/Hz under indoor conditions (a slow fading environment). Therefore this technology can find application in the emerging high-speed fixed Broadband Wireless Access (BWA) and Wireless Local Loop (WLL) networks. The various diversity techniques can exploit multipath propagation effects for better communication.

It is known that, only limited empirical data and channel models exists for a MIMO configuration [19,20], where the channel coefficients are arranged in a matrix form, popularly called the 'H' matrix and therefore measurements and characterization of a MIMO channel is of paramount importance.

A 2×2 MIMO channel can be implemented in hardware using microstrip antennas, which should be capable of registering measurements for different kinds of channel set-up, including different multi-path situations for indoor and outdoor conditions. This system should also be able to take long-term or multiple-hours measurements. A set-up as given in the figure(5.4) can be used, almost similar to the one suggested in [19]. A static transmit-antenna and mobile receive-antenna would be suitable.The

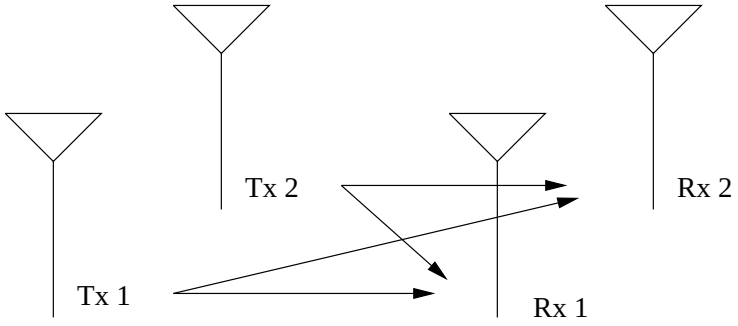

Figure 5.4: A 2 x 2 MIMO set-up

spatial diversity can be generated either by using many antennas or by using dual-polarised antennas or both. A lot of empirical data can be accumulated using these kinds of set-ups, and this data may help in realizing the full potential of space-time diversity.

Chapter 6

Conclusion

A dual shorting-pin microstrip antenna operating at 880MHz was designed and fabricated. The design and simulation of this antenna has been carried out using the Finite Difference Time Domain technique. FDTD technique was used as the formulation of the discretized equations is simple, and it is also well-suited for applications such as design of antennas. An implementation of FDTD method simulates the return loss and the radiation patterns to a high degree of accuracy. This dual shorting-pin microstrip antenna was fabricated and the results measured compare well with the simulated values. These antennas, when used as elements in a multiple antenna system, enables the system achieve an improvement in channel capacity, besides imparting the ability of dynamic beam-steering.

Bibliography

[1] S. Eisenberg, D. Muldoon,
"http://www.bell-labs.com/news/1998/september/9/2.html," Bell Labs Media Release, september 1998.

[2] E. Telatar, "Capacity of Multi-antenna Gaussian Channels", *IEEE Trans. Commun.*, vol. 42, No. 2/3/4, pp. 1617–1627, November-December 1999.

[3] J.H.Winters, J. Salz, G.D. Gitlin, "The capacity of wireless communication systems," *1st International Conference on Universal Personal Communications,92 Proc.,* 1992, pp. 02.01/1 -02.01/5.

[4] A. Taflove, " Computational Electrodynamics : the finite difference time-domain method," Norwood MA:, Artech House. 1996.

[5] D. Sullivan, " An unsplit step 3D PML for use with the FDTD method, *IEEE Microwave Guided Wave Lett.,* vol. 7, pp. 184186, July 1997.

[6] J. P. Berenger, "A perfectly matched layer for the absorption of electro-magnetic waves, *J. Comput. Phys.,* vol. 114, pp. 185200, 1994.

[7] G. Lazzi, O. P. Gandhi, D. M. Sullivan, "Use of PML absorbing layers for the truncation of the head model in cellular telephone simulations," *Microwave Theory and Techniques, IEEE Transactions on ,* Vol. 48 Issue. 11 Part. 2 , Nov. 2000, pp. 2033 -2039.

[8] G. Mur, "Absorbing Boundary Conditions for the Finite-Difference Approximation of the Time Domain Electromagnetic Field Equations," *IEEE Trans. Electromagnetic Compatibility*, Vol. 23, No. 4, November 1981.

[9] R. B. Waterhouse, S. D. Targonski,D. M. Kokotoff, " Design and performance of small printed anetnnas," *IEEE Trans on Ant. and Prop.,* Vol. 46, Issue. 11 , Nov. 1998, pp. 1629 -1633.

[10] R. B. Waterhouse " Small microstrip patch antenna," *Electronics Letters,* Vol. 31 Issue. 8 , 13 April 1995, pp. 604 -605.

[11] M. Sanad, " Effect of the shorting posts on short circuit microstrip antennas," *Proc.IEEE Antennas Propagat. Symp.,* Seattle, WA, June 1994, pp. 794-797.

[12] M. Sanad, "Microstrip antennas on very small ground planes for portable communication systems," *Antennas and Propagation Society International Symposium, 1994. AP-S. Digest,* Vol. 2 , 1994 , pp. 810 -813.

[13] H. K. Kan and R. B. Waterhouse, "Size reduction technique for shorted patches, *Electronics Letters,* Vol. 35, pp. 948 - 949, Jun. 1999.

[14] R. J. Luebbers, H. S. Langdon, "A simple feed model that reduces time steps needed for FDTD antenna and microstrip calculations," *IEEE Trans. on Ant. and Prop.,*Vol. 44, Issue. 7, July 1996, pp. 1000 -1005

[15] D. Sievenpiper, L. Zhang , R. F. J. Broas, N. G. Alexopolous, E. Yablonovitch, "High-impedance electromagnetic surfaces with a forbidden frequency band," *IEEE Trans. MTT,* Vol. 47 Issue. 11 , Nov. 1999, pp. 2059 -2074.

[16] E. Yablonovitch, "High-impedance electromagnetic ground planes ," *Microwave Symposium Digest, 1999 IEEE MTT-S International,* Vol. 4 , 1999, pp. 1529 -1532 vol.4.

[17] D. Sievenpiper, R. F.J Broas, E. Yablonovitch, "Antennas on high-impedance ground planes," *Microwave Symposium Digest, 1999 IEEE MTT-S International,* Vol. 3 , 1999, pp. 1245 -1248 vol.3.

[18] G. D. Golden, G. J. Foschini, R. A. Valenzuela, P. W. Wolniansky, Detection algorithm and initial laboratory results using the V-BLAST space-time communication architecture," *Electron. Lett.,* vol. 35, no. 1,pp. 1415, Jan. 1999.

[19] B. S. Baum, D. Gore, R. Nabar, S. Panchanathan, K. V. S. Hari, V. Erceg, A. J. Paulraj, "Measurement and characterization of broadband MIMO fixed wireless channels at 2.5 GHz," *IEEE Intern. Conf. Personal Wireless Communications,* pp.203 -206, 2000.

[20] L. J. Greenstein, D. G. Michelson, V. Erceg, "Moment-Method Estimation of the Ricean K-Factor," *IEEE Communications Letters,* vol. 3, no. 6, 1999.

[21] I.J.Bahl , P.Bhartia, "Microstrip Antennas," Artech House. 1980

[22] C. A. Balanis, "Antenna Theory, Analysis and Design," John Wiley and sons. 1982.

[23] R. E. Collin, "Antennas and Radiowave Propagation," McGraw Hill. 1985.

[24] D. E. Cheng, "Fundamentals of Engineering Electromagnetics," Addison-Wesley Publishing Company. 1993.

[25] M. N.O. Sadiku, "Numerical techniques in electromagnetics," Boca Raton, Fla. , CRC Press, c1992.

[26] K. Hirasawa, M. Haneishi, "Analysis, Design, and Measurements of Small and Low-Profile Antenna," Norwood, Artech House. 1992.

[27] T. S. Rappaport, "Wireless Communications, Principle and Practice," Prentice Hall, 1996.

[28] G. J. Foschini, "Layered space-time architecture for wireless communication in a fading environment when using multi-element antennas," *Bell Labs Tech. J.*, vol. 1, no. 2, pp. 41-59, Aug. 1996.

[29] P. W. Wolniansky, G. J. Foschini, G. D. Golden, R. A. Valenzuela, "V-BLAST: an architecture for realizing very high data rates over the rich-scattering wireless channel ," *URSI International Symposium on Signals, Systems, and Electronics, 1998,* ISSSE 98., 1998, pp. 295 -300